

archives
of thermodynamics

Vol. 41(2020), No. 2, 223–238

DOI: 10.24425/ather.2020.133630

Heat and mass transfer mechanism on three-dimensional flow of inclined magneto Carreau nanofluid with chemical reaction

B. MADHUSUDHANA RAO^a
DEGAVATH GOPAL^b
NAIKOTI KISHAN^b
SAAD AHMED^a
PUTTA DURGA PRASAD^{*c}

^a Lecturer in Mathematics, Higher College of Technology (IT), Muscat, Oman-133

^b Department of Mathematics, UCS, Osmania University, Hyderabad, TS-500007, India

^c Department of Mathematics, SAS, Vellore Institute of Technology, Chennai, TN-600127, India

Abstract The characteristic of nano sized particles mass flux conditions are engaged in this investigation. Here we assume that the nano sized particle flux is zero and the nano sized particle fraction arranged itself on the boundary layer. With this convincing and revised relation, the features of Buongiorno relation on three-dimensional flow of Carreau fluid can be applied in a more efficient way. The governing partial differential equations of continuity, momentum, energy and concentration equations which are transmitted into set of pair of nonlinear ordinary differential equations utilizing similar transformations. The numeric solutions are acquired by engaging the bvp4c scheme, which is a finite-difference code for solving boundary value problems. A parametric study is accomplished to demonstrate the impact of Prandtl number, Weissenberg numbers, radiation parameter, chemical reaction parameter, thermophoresis parameter, Brownian motion parameter and Lewis number on the fluid velocity, temperature and concentration profiles as well skin friction coefficient, Nusselt number and Sherwood number

*Corresponding Author. Email: durga.prsd@gmail.com

within the boundary layer. From this we find the way in which magnetic parameter contributes to the increase in local skin fraction, and the decrease in the Nusselt and Sherwood numbers in these cases. The effects of the velocity temperature and concentration profile are obtained and presented graphically.

Keywords: Carreau nanofluid; Chemical reaction; MHD; Heat and mass transfers

Nomenclature

a, b	– positive constants
B_0	– strength of the magnetic field
C	– concentration of the nanofluid
C_∞	– free stream concentration of the nanofluid
C_f	– skin friction coefficient
D_B, D_T	– Brownian and thermophoresis diffusion coefficients
f, g	– dimensionless components of velocity
k_0	– chemical reaction coefficient
k^*	– mean absorption coefficient
Le	– Lewis number
M	– magnetic field parameter
Nb	– Brownian motion parameter
Nt	– thermophoresis parameter
Nu	– Nusselt number
n	– power law exponent
Pr	– Prandtl number
q_r	– radiative heat flux
q_w	– mass flux
R	– radiation parameter
Re	– Reynolds number
Sh	– Sherwood number
T	– temperature of the nanofluid
T_∞	– free stream temperature of the nanofluid
u, v, z	– velocity components in x, y and z directions
We_1, We_2	– Weissenberg numbers
x, y, z	– Cartesian coordinates

Greek symbols

α	– inclination of the stretching sheet parameter
α_1	– thermal conductivity

- α_1 – stretching ratio parameter
- β – Casson fluid parameter
- Γ – material rate constant
- η – dimensionless variable
- θ – dimensionless temperature
- ν – kinematic viscosity
- ρ – density of the fluid
- σ – electric conductivity
- σ^* – Stefan-Boltzmann constant
- τ – chemical reaction parameter
- ϕ – dimensionless concentration

Subscripts

- ∞ – condition at the free stream
- f – dimensionless velocity
- w – condition at the free surface

1 Introduction

Present modern nanotechnology offers preparation of nanometer sized particles or nanostructured engineering materials on the atomic or molecular scales with enhanced thermophysical properties, if compared to their respective larger forms. These nanoparticle-fluid suspensions are termed nanofluids, obtained by dispersing nanometer sized particles in a conventional base fluid like water, oil, ethylene glycol, etc. Historically it was Choi and Eastman [1] who provided ideas of how to make suspensions of the fluid and nano-sized particles and named such mixture a nanofluid. One can find further applications related to nanofluids in [2].

Nanoparticles of materials such as metallic oxides (Al_2O_3 , CuO), nitride ceramics (AlN , SiC), carbide ceramics (SiC , TiC), metals (Cu , Ag , Au), etc. have been used for the preparation of nanofluids. These nanofluids have been developed to possess an enhanced thermal conductivity as well as improved heat transfer performance at low concentrations of nanoparticles. Even at very low volume fractions of the suspended particles, an attractive enhancement in thermal conductivity has been reported on these nanoparticle based fluids. For instance, numerous exhausting investigations [3–6] have established an escalation in the thermal conductivity of ordinary fluids containing the nanoparticles. Nowadays the non-Newtonian fluid [7–11] acquires a new courtesy because of its strong use in industrial applications, mostly in chemical engineering processes and polymer processing. Owing to this significance of non-Newtonian fluids in 1944 Powell and Eyring anticipated a novel fluid model known as the Eyring-Powell fluid model [12].

The studies formerly cited ultimately stress that the condition of three-dimensional boundary layer flow is not well renowned for such fluids. Our concern in the simultaneous analysis is to argue the influence of non-linear radiative flow on the magnetohydrodynamic (MHD) three-dimensional flow of Eyring-Powell fluid [13–14]. The chemical reaction stimulates a great role in the investigation involving heat and mass transfer in areas of science and engineering technology as result of wide coverage of industrial applications [15], entropy generation analysis for peristalsis of nanofluid with Ohmic heating, temperature dependent viscosity and Hall effects [16], numerical analysis of nanofluid flow in permeable media under the effect of external magnetic source [17], and non-uniform heat source/sink and multiple slips on three-dimensional magnetic-Casson fluid in a suspension of copper nanoparticles over a porous slendering sheet [18].

A chemical reaction between the conventional fluid and nanoparticles are classified as a homogeneous reaction during a given phase or heterogeneous reaction that is surrounded by a boundary of the phase. Reaction rate in a first-order chemical reaction is directly related to the concentration. In view of the pertinent applications, several authors have considered and collected their results of chemical reaction effects on the flow of heat and mass transfer with different geometries [19–21].

In Carreau model, the viscosity depends upon the shear rate. This is introduced by Carreau, using the Cauchy's equation involving the extra stress tensor for the 'Carreau fluid' [24]. Additionally, the power-law of Carreau fluid is also the one of the non-Newtonian fluids. Carreau fluid model is valid for viscous, high and low shear rates. Because of this advancement, it has benefited in many technological and manufacturing flows. With that in mind, the mass transfer characteristics of Carreau fluid over a swarm of Newtonian drop was scrutinized in [25]. The time dependent Poiseuille flow of Carreau fluid in the presence of slip effect was investigated in [26] and it was concluded that the wavelength and amplitude of oscillations in radial direction are decreasing with the increase in the slip effect. The peristaltic flow characteristics of Carreau fluid in the uniform tube was discussed in terms of the heat transfer characteristics of Carreau fluid in [27].

In view of these facts the present investigation focuses on the three-dimensional flow of magnetohydrodynamic Carreau fluid in presence of chemical reaction. The effect has been incorporated into the proposed mathematical model. The boundary layer equations given as a set of partial differential equations are first transformed into a non-linear ordinary

differential equations and subsequently solved numerically using the Runge-Kutta method. The effects of the governing flow parameters on the velocity, temperature and concentration profiles have been discussed and presented in graphs.

2 Mathematical formulation of the model

We ponder the steady three-dimensional electrically conducting forced convective Carreau nanofluid over a bidirectional stretched surface. The flow is induced owing to stretching surface in two horizontal x - and y -axis directions with velocity $u^{1/4}ax$ and $v^{1/4}by$, respectively, where a and b are stretching rates and the fluid flow occupies the region in the domain $z > 0$. The transverse magnetic field of strength B_0 is imposed parallel to z -axis as revealed. It is also assumed that induced magnetic and electric fields are insignificant when compared to the applied magnetic field. This postulate is effective only for the insignificant magnetic Reynolds number range. Temperature of the nanofluid at the surface T_w is superior to temperature of nanofluid distant from the stretched surface. The Carreau nanofluid relation in view of overhead declared assumptions is given below:

$$u_x + v_y + w_z = 0, \quad (1)$$

$$uu_x + vv_y + ww_z = \nu u_{zz} \left[1 + \Gamma(u_z)^2 \right]^{\frac{n-1}{2}} + \nu(n-1)\Gamma^2(u_z)^2 u_{zz} \left[1 + \Gamma^2(u_z)^2 \right]^{\frac{n-3}{2}} - \frac{\sigma B_0^2}{\rho_f} u \sin^2 \alpha, \quad (2)$$

$$vv_x + vv_y + ww_z = \nu v_{zz} \left[1 + \Gamma(v_z)^2 \right]^{\frac{n-1}{2}} + \nu(n-1)\Gamma^2(v_z)^2 v_{zz} \left[1 + \Gamma^2(v_z)^2 \right]^{\frac{n-3}{2}} - \frac{\sigma B_0^2}{\rho_f} v \sin^2 \alpha, \quad (3)$$

$$uT_x + vT_y + wT_z = \alpha_1 T_{zz} + \tau \left[D_B C_z T_z + \frac{D_T}{T_\infty} (T_z)^2 \right] - \frac{1}{(\rho c)_f} (q_r)_z, \quad (4)$$

$$uC_x + vC_y + wC_z = D_B C_{zz} + \frac{D_T}{T_\infty} T_{zz} - k_0 (C - C_\infty). \quad (5)$$

The boundary conditions suitable to the present flow problem are

$$u = ax = U_w(x), \quad v = by = V_w(y), \quad w = 0, \quad T = T_w,$$

$$D_B C_z + \frac{D_T}{T_\infty} T_z = 0 \text{ as } z \rightarrow 0, u \rightarrow 0, v \rightarrow 0, T \rightarrow T_\infty, C \rightarrow C_\infty \text{ as } z \rightarrow \infty. \quad (6)$$

The Rosseland approximation for radiation is given below

$$(q_r)_z = -\frac{4\sigma^*}{3k^*} T_z^4. \quad (7)$$

It is assumed that the temperature differences within the flow, such as the term T^4 , are expressed as a linear function of temperature. The Taylor series expansion for T^4 about a free stream temperature T_∞ after neglecting higher order terms yields

$$T^4 = 4T_\infty^3 T - 3T_\infty^4. \quad (8)$$

Using Eqs. (7) and (8), we obtain

$$(q_r)_z = -\frac{16\sigma^* T_\infty^3}{3k^*} T_{zz}. \quad (9)$$

By incorporation of the Rosseland approximation (Brewster [22]), the energy, Eq. (4), can be cast into the form

$$uT_x + vT_y + wT_z = \alpha_1 T_{zz} + \tau \left[D_B C_z T_z + \frac{D_T}{T_\infty} (T_z)^2 \right] + \frac{16\sigma^* T_\infty^3}{3(\rho c)_f k^*} T_{zz}. \quad (10)$$

Introducing the definitions of velocity components $u = axf_\eta(\eta)$, $v = ayg_\eta(\eta)$, $w = -(a\nu)^{0.5} [f(\eta) + g(\eta)]$, the non-dimensional transformation variables are obtained:

$$\theta(\eta) = \frac{T - T_\infty}{T_w - T_\infty}, \quad \phi(\eta) = \frac{C - C_\infty}{C_w - C_\infty}, \quad \eta = z \left(\frac{a}{\nu} \right)^{0.5}. \quad (11)$$

Equations (2), (3), (5), and (10) reduce to the relations:

$$f_{\eta\eta\eta} \left[1 + \text{We}_1^2 (f_{\eta\eta})^2 \right]^{\frac{n-3}{2}} \left[1 + n \text{We}_1^2 (f_{\eta\eta})^2 \right] - (f_\eta)^2 + f_{\eta\eta} (f + g) - M^2 f_\eta \sin \alpha = 0, \quad (12)$$

$$g_{\eta\eta\eta} \left[1 + \text{We}_2^2 (g_{\eta\eta})^2 \right]^{\frac{n-3}{2}} \left[1 + n \text{We}_2^2 (g_{\eta\eta})^2 \right] - (g_\eta)^2 + g_{\eta\eta} (f + g) - M^2 g_\eta \sin \alpha = 0, \quad (13)$$

$$\left(1 + \frac{4R}{3}\right) \theta_{\eta\eta} + \text{Pr}(f + g) \theta_{\eta} + \text{Pr}Nb\theta_{\eta}\phi_{\eta} + \text{Pr}Nt\theta_{\eta}^2 = 0, \quad (14)$$

$$\phi_{\eta\eta} + \text{LePr}(f + g) \phi_{\eta} + \left(\frac{Nt}{Nb}\right) \theta_{\eta\eta} - \text{LePr}\tau' \phi = 0. \quad (15)$$

The corresponding boundary conditions are

$$\begin{aligned} f(\eta) = 0, \quad g(\eta) = 0, \quad f'(\eta) = 1, \quad g'(\eta) = \alpha_1, \quad \theta(\eta) = 1, \\ Nb\phi'(\eta) + Nt\theta'(\eta) = 0 \quad \text{as } \eta \rightarrow 0, \quad f'(\eta) \rightarrow 0, \\ g'(\eta) \rightarrow 0, \quad \theta(\eta) \rightarrow 0 \quad \text{as } \eta \rightarrow \infty, \end{aligned} \quad (16)$$

$$\text{We}_1 = \left(\frac{\Gamma^2 a U_w^2}{\nu}\right)^{0.5}, \quad \text{We}_2 = \left(\frac{\Gamma^2 a V_w^2}{\nu}\right)^{0.5}, \quad M = \left(\frac{\sigma B_0^2}{\rho_f a}\right),$$

$$R = \frac{4\sigma^* T_{\infty}^3}{k^* k}, \quad Nb = \frac{D_B \tau (C_w - C_{\infty})}{\nu}, \quad Nt = \frac{D_T \tau (T_w - T_{\infty})}{T_{\infty} \nu},$$

$$\tau' = \frac{k_0}{a}, \quad \text{Le} = \frac{\gamma}{D_B}, \quad \text{Pr} = \frac{\nu}{\gamma}, \quad \alpha_1 = \frac{b}{a}.$$

The physical point of interest is the expressions for the local skin friction coefficient, C_f , on the surface along the x - and y -axis directions, which are denoted by C_{f_x} and C_{f_y} . The local Nusselt number, i.e. the non-dimensional heat transfer coefficient and Sherwood numbers are defined as:

$$\begin{aligned} C_{f_x} = \frac{\tau_{xz}}{0.5\rho_f U_w^2}, \quad C_{f_y} = \frac{\tau_{yz}}{0.5\rho_f V_w^2}, \quad \text{Sh}_x = \frac{xq_w}{D_B(C_w - C_{\infty})}, \\ \text{Nu}_x = -\frac{x}{T_w - T_{\infty}} (T_z)_{z=0} + \frac{xq_r}{k(T_w - T_{\infty})}. \end{aligned} \quad (17)$$

The non-dimensional form of the skin friction, Nusselt number, and Sherwood number are given below:

$$0.5C_{f_x} \text{Re}_x^{0.5} = f_{\eta\eta}(0) \left[1 + \text{We}_1^2 f_{\eta\eta}^2(0)\right]^{\frac{n-1}{2}},$$

$$0.5C_{f_y} \text{Re}_x^{0.5} = g_{\eta\eta}(0) \left[1 + \text{We}_2^2 g_{\eta\eta}^2(0)\right]^{\frac{n-1}{2}},$$

$$\text{Re}_x^{-0.5} \text{Nu}_x = -\left(1 + \frac{4R}{3}\right) \theta_{\eta}(0), \quad \text{Re}_x^{-0.5} \text{Sh}_x = -(\phi_{\eta}(0)). \quad (18)$$

Here τ_{xz} and τ_{yz} are the wall shear stresses along x - and y -axis directions, whereas $\text{Re}_x = \frac{Ux}{\nu}$ and $\text{Re}_y = \frac{Vy}{\nu}$ are the local Reynolds numbers in x - and y -axis directions.

3 Results and discussion

The foremost attention of this section is to inspect the features of new mass flux conditions for the three-dimensional magnetohydrodynamic flow of Carreau nanofluid over a bidirectional stretching surface. For the sake of numerical computations, the finite-difference code for solving boundary value problems `bvp4c` has been applied for the exploration of the numerical parameters on the velocity components, temperature and concentration field.

The graphs are presented in the further showing the influences of various parameters on velocity components. Finally the local skin friction and the local Nusselt number are deliberated in detail. Figure 1 plotted to envisage the characteristics of the magnetic field parameter on the nanofluid velocity components $f'(\eta)$ and $g'(\eta)$ for shear thinning and shear thickening fluid. Since magnetic field specifies the fraction of viscous force to hydro-magnetic force, improvement in magnetic field parameter causes strength in hydromagnetic body force which trends to decelerate the fluid motion. Consequently, the collisions between the nanoparticles boosts, this mechanism reduces the associated momentum boundary layer. Therefore, the velocity of the nanofluid declines.

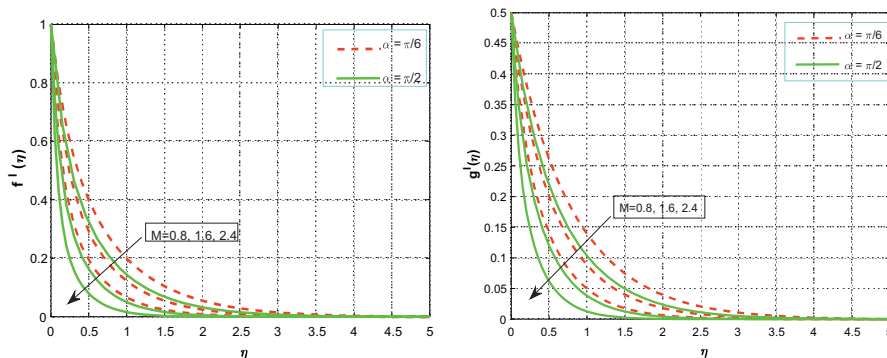


Figure 1: Influence of the magnetic field parameter M on velocity components $f'(\eta)$ and $g'(\eta)$.

Figure 2 is depicted to investigate the characteristics of magnetic parameter on the temperature and concentration distributions. It is found that large values of magnetic field M increase the temperature and concentration profiles, as magnetic field presents a force.

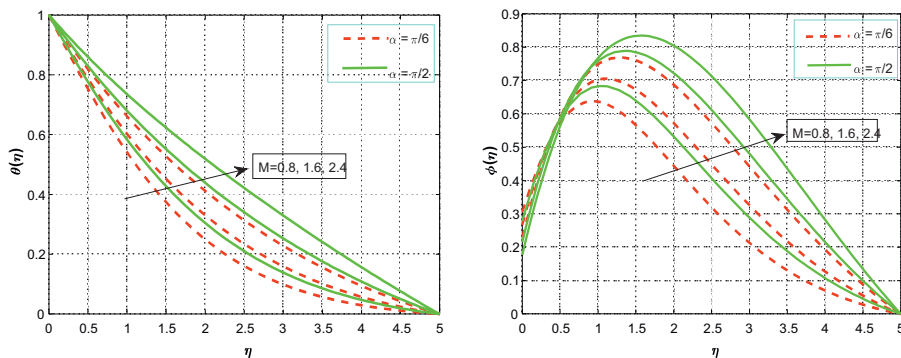


Figure 2: Influence of the magnetic field parameter M on temperature $\theta(\eta)$ and concentration $\phi(\eta)$ profiles.

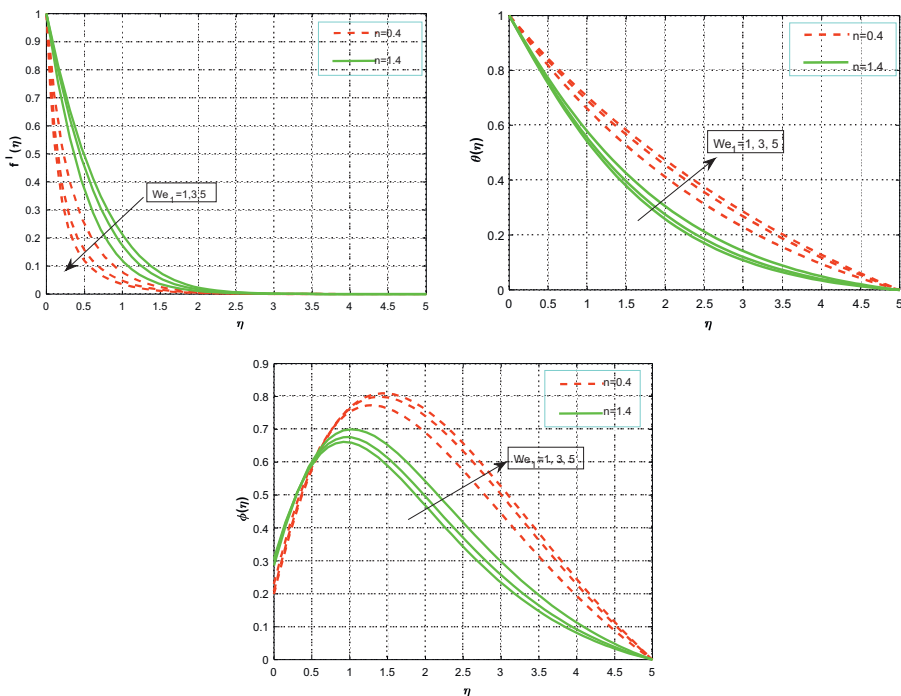


Figure 3: Influence of the Weissenberg number We_1 on velocity components $f'(\eta)$, and temperature $\theta(\eta)$ and concentration $\phi(\eta)$ profiles.

From Fig. 3 it is noticed that velocity decreases, temperature and concentration increase with the increase in Weissenberg number for $n = 0.4$ and 1.4.

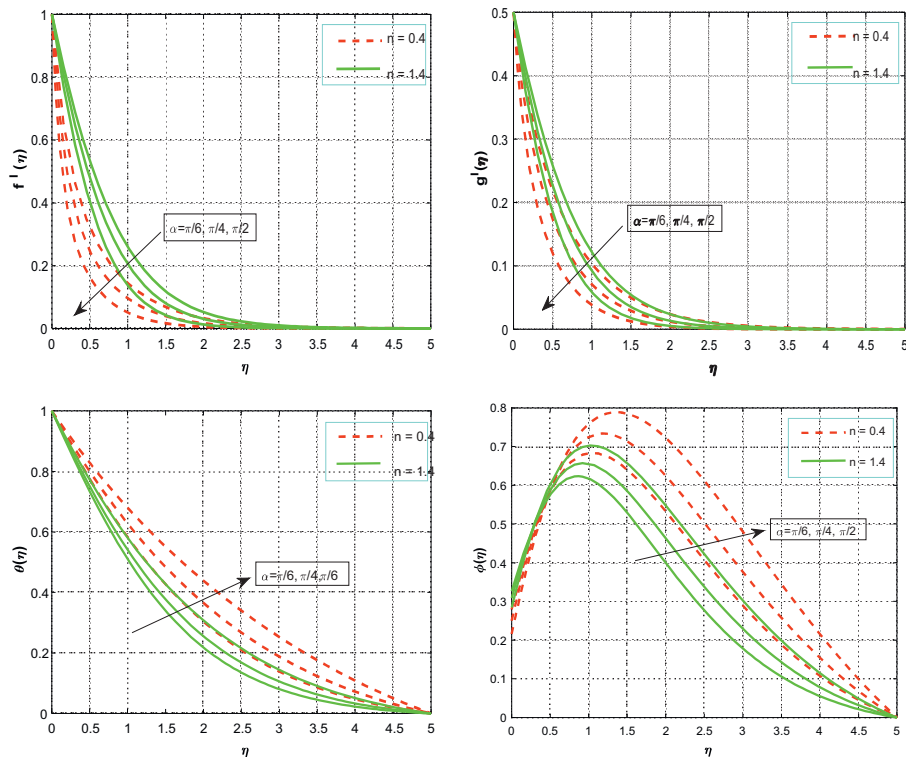


Figure 4: Influence of the inclination of the stretching sheet parameter α on velocity components $f'(\eta)$ and $g'(\eta)$ and temperature $\theta(\eta)$ and concentration $\phi(\eta)$ profiles.

From Fig. 4 it is observed that the nanofluid velocity components $f'(\eta)$ and $g'(\eta)$ and for shear thinning and shear thickening fluid decrease, nanofluid temperature and concentration components increase with the increase in inclination of the stretching sheet parameter (α) for $n = 0.4$ and 1.4. From Fig. 5 it is seen that nanofluid temperature and concentration components for shear thinning and shear thickening fluid are decreasing with the increase in Prandtl number (Pr). From Fig. 6 it is noticed that the nanofluid temperature increases and nanofluid concentration decreases for shear thinning and shear thickening fluid with the increase in radiation parameter (R). From Fig. 7 it is noticed that the nanofluid temperature and concentra-

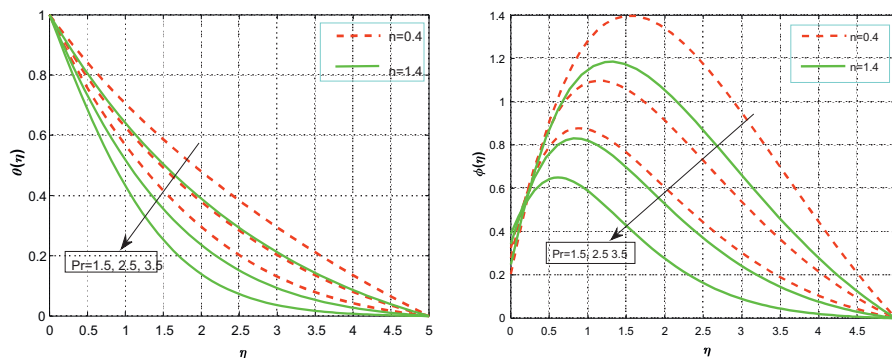


Figure 5: Influence of the Prandtl number Pr on temperature $\theta(\eta)$ and concentration $\phi(\eta)$ profiles.

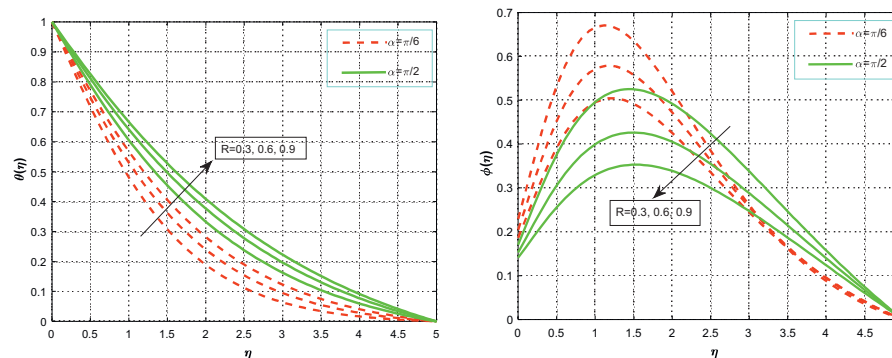


Figure 6: Influence of the radiation parameter R on temperature $\theta(\eta)$ and concentration $\phi(\eta)$ profiles.

tion components decrease for shear thinning and shear thickening fluid with the increase in chemical reaction. The effect of thermophoresis parameter (Nt) and Lewis number (Le) on concentration distributions is plotted in Figs. 8a and 8b. It is clear that all the profiles (concentration) decrease in the corresponding thermophoresis parameter and Lewis number. Figure 8c shows that the solute boundary layer thickness increases with the increase in Brownian motion parameter Nb . Note that the Brownian motion of the nanoparticles induces convection which increases the thermal conductivity of nanoparticles. So, higher the Brownian motion causes to enhance the temperature field.

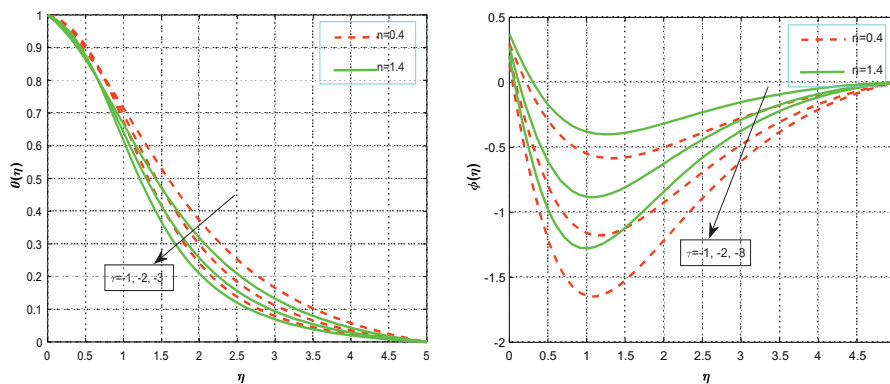


Figure 7: Influence of the chemical reaction parameter τ on temperature $\theta(\eta)$ and concentration $\phi(\eta)$ profiles.

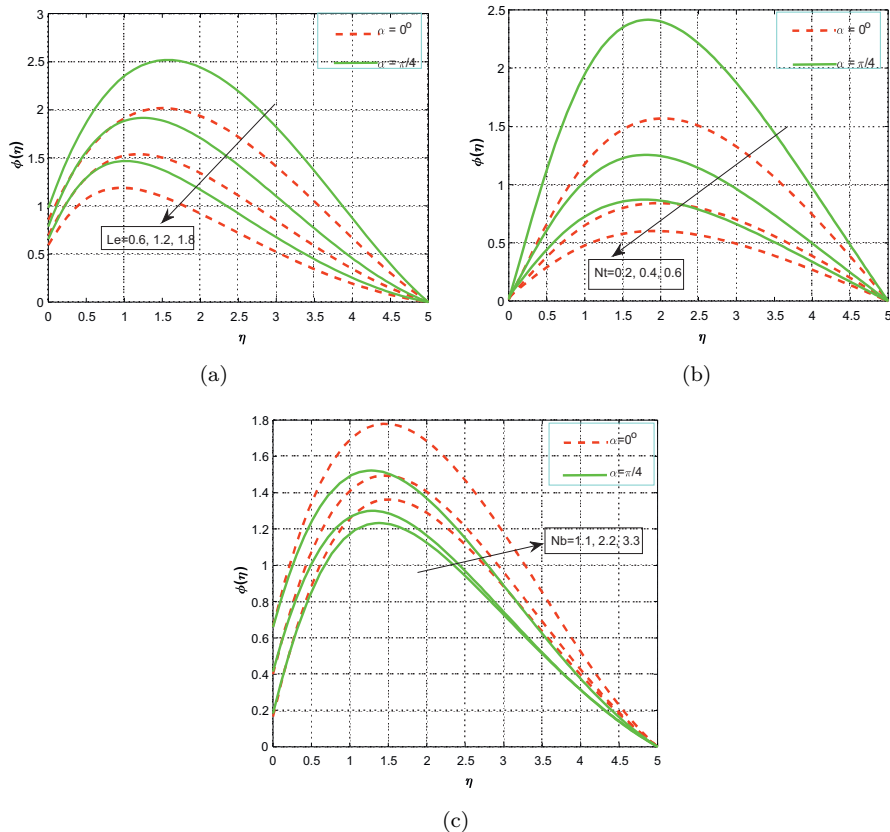


Figure 8: Influence of the Lewis number Le (a), thermophoresis parameter Nt (b), and Brownian motion parameter Nb (c) on concentration $\phi(\eta)$ profile.

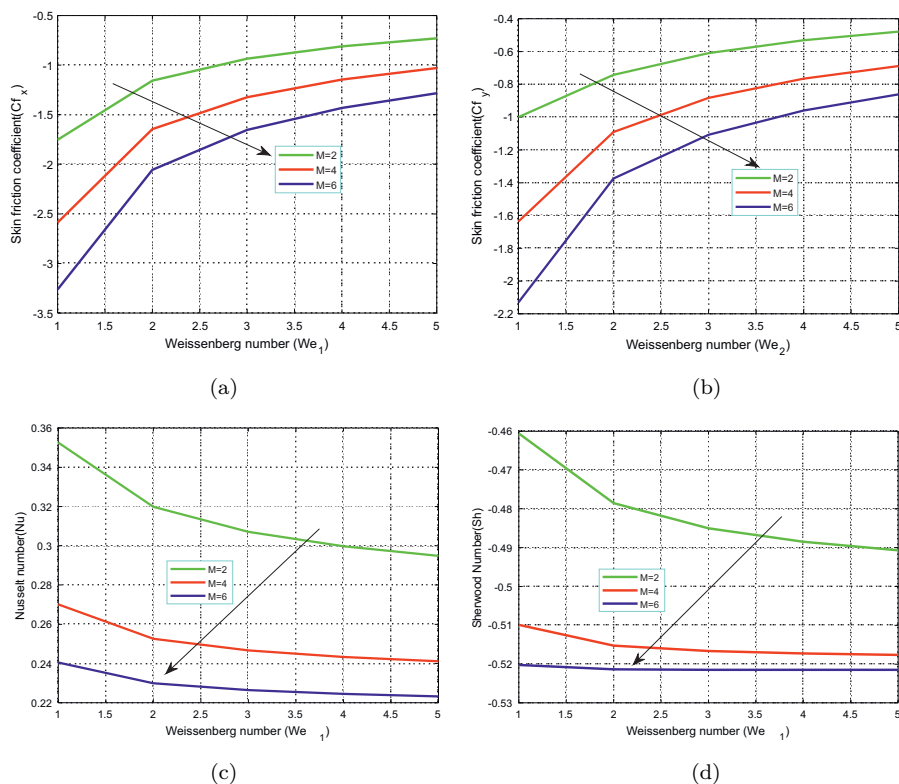


Figure 9: Influence of the magnetic field parameter M on skin friction coefficient C_f (a) and (b), Nusselt number (c), and Sherwood number (d) *versus* the Weissenberg number.

Figures 9a–d show the characteristics of magnetic field parameter for skin friction, Nusselt number and Sherwood number in function of the Weissenberg number. From these figures we observe that the increase in the magnetic field parameter causes the decrease in the friction factor, heat and mass transfer rates.

In order to test the accurateness of our present investigation we have calculated $-\theta'(0)$ for various values of Nt and compared with Khan and Pop [23] by considering the situation in absence of magnetic field parameter, Lewis number, Brownian motion parameter, radiation parameter. Table 1 is a comparison with Khan and Pop numerical results which shows a good agreement with the present work.

Table 1: Comparison of different values of physical parameter and fixed parameters when $M = We_1 = Le = R = Nb = 0, Pr = 10$ and $\alpha = \pi/2$.

Nt	Khan and Pop [23]	Present results
0.1	0.9524	0.952433
0.2	0.6932	0.693212
0.3	0.5201	0.520149
0.4	0.4026	0.402633
0.5	0.3211	0.321152

4 Conclusions

Due to numerous applications of three-dimensional flow in manufacturing processes like super capacitors, water desalination, lithium ion batteries and fuel cells in this study, we examined the heat and mass transfer effects on three-dimensional magneto Carreau fluid in the presence of chemical reaction. The Runge-Kutta method has been employed to resolve the altered governing non-linear equations and results are presented through the graphs. The following points are worth mentioning.

- The magnetic field parameter causes to decrease the velocity distribution.
- Chemical reaction parameter decelerates the temperature and concentration profiles.
- The angle of inclination reduces the velocity distributions for various values of $n = 0.4$ and $n = 1.4$.
- The magnetic field parameter decelerates the friction factor rates along with local Weissenberg numbers and also reduces the heat and mass transfer rates.
- The Brownian motion parameter improves the mass transfer rate.
- Lewis number and thermophoresis parameters are decreasing the rate of mass transfer rate.

References

- [1] CHOI S.U.S., EASTMAN J.A.: *Enhancing thermal conductivity of fluids with nanoparticles*. In: Proc. ASME Int. Mechanical Engineering Cong. Exp. San Francisco, Nov. 12-17, 1995.
- [2] WONG K.V., LEON O.: *Applications of nanofluids: Current and future*. Adv. Mech. Eng. **2**(2010), 519659.
- [3] Eastman J., Choi S., Li S., Yu W., Thompson L.: *Anomalously increased effective thermal conductivities of ethylene glycol based nanofluids containing copper nanoparticles*. Appl. Phys. Lett. **78**(2001), 7, 18–20.
- [4] DAS S., PUTRA N., ROETZEL W.: *Pool boiling characteristics of nano-fluids*. Int. J. Heat Mass Transf. **46**(2003), 8, 51–62.
- [5] BUONGIORNO J.: *Convective transport in nanofluids*. J. Heat Transf.-T. ASME **28**(2006), 2, 40–50.
- [6] JAIN S., PATEL H., DAS S.P.: *Brownian dynamic simulation for the prediction of effective thermal conductivity of nanofluid*. J. Nanopart Res. 11(2009), 7, 67–73.
- [7] KHAN M., HASHIM, ALSHOMRANI A.S.: *MHD stagnation-point flow of a Carreau fluid and heat transfer in the presence of convective boundary conditions*. PLOS ONE. 2016.
- [8] MAHANTHESHA B., GIREESHAB B.J., GORLA R.S.R.: *Unsteady three-dimensional MHD flow of a nano Eyring-Powell fluid past a convectively heated stretching sheet in the presence of thermal radiation, viscous dissipation and Joule heating*. J. Assoc. Arab. Uni. Basic App. Sci. **23**(2017), 75–84.
- [9] HASHIM, KHAN M., ALSHOMRANI A.S.: *Characteristics of melting heat transfer during flow of Carreau fluid induced by a stretching cylinder*. Eur. Phys. J. E **40**(2017), 8. <http://dx.doi.org/10.1140/epje/i2017-11495-6>
- [10] HAYAT T., KHAN M.I., WAQAS M., ALSAEDI A.: *Effectiveness of magnetic nanoparticles in radiative flow of Eyring-Powell fluid*. J. Mol. Liq. **231**(2017), 126–133.
- [11] HAYAT T., SAJJAD R., MUHAMMAD T., ALSAEDI A., ELLAHI R.: *On MHD nonlinear stretching flow of Powell-Eyring nanomaterial*. Results Phys. **7**(2017), 535–543.
- [12] POWELL R.E., EYRING H.: *Mechanisms for the relaxation theory of viscosity*. Nature **154**(1944), 427–428.
- [13] EL DABE N.T.M., HASSAN A.A., MOHAMED M.A.A.: *Effect of couple stresses on the MHD of a non-Newtonian unsteady flow between two parallel porous plates*. Z. Naturforsch. a **58**(2003), 204–210.
- [14] PATEL M., TIMOL M.G.: *Numerical treatment of Powell-Eyring fluid flow using method of satisfaction of asymptotic boundary conditions (MSABC)*. Appl. Numer. Math. **59**(2009), 10, 84–92.
- [15] HAYAT T., WAQAS M., SHEHZAD S., ALSAEDI A.: *Chemically reactive flow of third grade fluid by an exponentially convected stretching sheet*. J. Mol. Liq. **223**(2016), 853–860.

- [16] HAYAT T., ZUBAIR M., WAQAS M., ALSAEDI A., AYUB M.: *Importance of chemical reactions in flow of Walter-B fluid subject to non-Fourier flux modeling*. J. Mol. Liq. **238**(2017), 229–235.
- [17] ABBASI F.M., SHANAKHAT I., SHEHZAD S.A.: *Entropy generation analysis for peristalsis of nanofluid with Ohmic heating, temperature dependent viscosity and Hall effects*. J. Magn. Magn. Mater. **474**(2019), 434–441.
- [18] SHEIKHOLESAMI M., SHEHZAD S.A.: *Numerical analysis of Fe₃O₄-H₂O nanofluid flow in permeable media under the effect of external magnetic source*. Int. J. Heat Mass Transf. **118**(2018), 182–192.
- [19] SEKHAR K.R., REDDY G.V., RAJU C.S.K., SHEHZAD S.A.: *Non-uniform heat source/sink and multiple slips on 3D magnetic-Casson fluid in a suspension of copper nanoparticles over a porous slendering sheet*. J. Nanofluids (JON) **7**(2018), 3, 469–477.
- [20] HAYAT T., WAQAS M., SHEHZAD S., ALSAEDI A.: *On 2D stratified flow of an Oldroyd-B fluid with chemical reaction: an application of non-Fourier heat flux theory*. J. Mol. Liq. **223**(2016), 566–571.
- [21] PONTES F.A., MIYAGAWA H.K., PONTES P.C., MACÊDO E.N., QUARESMA J.N.: *Integral transform solution of micropolar magnetohydrodynamic oscillatory flow with heat and mass transfer over a plate in a porous medium subjected to chemical reactions*. J. King Saud Univ.-Sci. **31**(2019), 1, 114–126.
- [22] BREWSTER M.Q.: *Thermal Radiative Ttransfer and Properties*. Wiley, New York 1992.
- [23] KHAN, W.A., POP, I.: *Boundary layer flow of nanofluid past a stretching sheet*. Int. J. Heat Mass Transf. **53**(2010), 11-12, 2477–2483.
- [24] RAJU C.S.K., SANDEEP N.: *Unsteady three-dimensional flow of Casson-Carreau fluids past a stretching surface*. Alexandria Eng. J. **55**(2016), 2, 1115–1126.
- [25] ZHU J.: *Drag and mass transfer for flow of a Carreau fluid past a swarm of Newtonian drops*. Int. J. Multiph. Flow **21**(1995), 935–940.
- [26] GEORGIU G.C.: *The time-dependent, compressible Poiseuille and extrudate-swell flows of a Carreau fluid with slip at the wall*. J. Non-Newtonian Fluid Mech. **109**(2003), 2-3, 93–114.
- [27] ABD EL NABY A.H., EI MISERY A.E.M., ABDEL KAREEM M.F.: *Separation in the flow through peristaltic motion of a Carreau fluid in uniform tube*. Physica A. **343**(2004), 2, 1–14.